

## A STUDY OF THE REACTION KINETICS OF $\text{SOCl}_2$ IN ELECTROLYTES CONTAINING $\text{AlCl}_3$ OR $\text{LiAlCl}_4$

J. G. CHIU, Y. Y. WANG and C. C. WAN

*Department of Chemical Engineering, Tsing-Hua University, Hsin-Chu, Taiwan (Republic of China)*

(Received November 5, 1986; in revised form February 15, 1987)

### Summary

The reaction mechanism of  $\text{SOCl}_2$  in electrolytes containing  $\text{AlCl}_3$  or  $\text{LiAlCl}_4$ , and the factors affecting the capacity of carbon electrodes in the  $\text{Li}/\text{SOCl}_2$  battery system have both been investigated.

The capacity of the carbon electrode is found to be dependent on its porosity, *i.e.*, the greater the porosity, the higher the capacity. The electrode porosity can be controlled both by the manufacturing pressure and by the addition of a PTFE binder. A pressure of  $10 \text{ kg cm}^{-2}$  and a PTFE content of 5 wt.% are found to give the best electrode performance.

A study of the reduction mechanism of  $\text{AlCl}_3/\text{SOCl}_2$  and  $\text{LiAlCl}_4/\text{SOCl}_2$  electrolytes on platinum has been conducted using cyclic voltammetry. The reactions are mass-transfer controlled and are irreversible when the scan rate is between 2 and 200 and 20 and 500  $\text{mV s}^{-1}$  for the  $\text{AlCl}_3/\text{SOCl}_2$  and  $\text{LiAlCl}_4/\text{SOCl}_2$  electrolytes, respectively. The diffusion coefficients are estimated to be  $10^{-6}$  and  $10^{-10} - 10^{-12} \text{ cm}^2 \text{ s}^{-1}$  for the  $\text{AlCl}_3/\text{SOCl}_2$  and  $\text{LiAlCl}_4/\text{SOCl}_2$  systems, respectively.

---

### Introduction

The  $\text{Li}/\text{SOCl}_2$  battery has attracted considerable attention in recent years [1]. Most of the research effort has been focussed on the carbon electrode, which is a key factor in controlling the capacity and discharge characteristics of the battery. For example, Marincic [2] has explored, from a theoretical point of view, the relationship between the performance of the battery and the structure of the electrode. From experimental studies, Dey [3] deduced the optimum conditions for both the electrolyte and the composition of the carbon electrode. Using both scanning electron microscopy and energy dispersive X-ray analysis, Szpak [4] has examined the characteristics of the carbon electrode in batteries discharged at high rates. Finally, the relationship between battery characteristics and the materials used in the construction of carbon electrodes has been investigated by Klinedinst [5].

The purpose of the work reported here is two-fold. First, the relationship between the capacity and the porosity of the carbon electrode is examined, and second, the reaction kinetics of  $\text{SOCl}_2$  in electrolytes containing  $\text{AlCl}_3$  or  $\text{LiAlCl}_4$  is studied.

## Experimental

### *Preparation of carbon electrodes [6]*

Shawinigan carbon black (supplied by Gulf Oil Chemicals Company; true density reported as  $1.95 \text{ g cm}^{-3}$ ) was soaked in acetone for 4 h and then rinsed with de-ionized water. After filtering, the carbon was placed in a vacuum oven held at  $100^\circ\text{C}$  for one day. The resultant carbon powder was mixed with a solution of 5 wt.%  $\text{KMnO}_4$  and 25 wt.%  $\text{KOH}$  for 1.5 h at  $50^\circ\text{C}$ . This solution was filtered and rinsed with de-ionized water and then dried under vacuum at  $100^\circ\text{C}$ .

A portion, 18 g, of the prepared carbon powder was added to 100 ml of ethyl alcohol/water solution (1:3 vol%). Then PTFE/water solutions (1.6 - 11.2 g) were added to form carbon pastes that contained 5 - 35% PTFE. The carbon pastes were dried under vacuum for two days at  $100^\circ\text{C}$ .

The prepared carbon paste (0.15 g) was applied to both sides of a  $3 \times 1.5 \times 0.2 \text{ cm}$  nickel screen. The electrode was subjected to a pressure in the range  $10 - 50 \text{ kg cm}^{-2}$ , at a temperature of  $370^\circ\text{C}$ . Carbon electrodes were stored under vacuum at  $100^\circ\text{C}$  prior to experimental studies.

The electrode was carefully weighed ( $W_A$ ) and put in a near-vacuum (below 30 mmHg) flask for 30 min. The flask was then filled with oil ( $80^\circ\text{C}$ ) and, after a further 30 min, air-cooled to room temperature. After absorbing oil, the electrode was again weighed in atmosphere ( $W_B$ ) and then in water ( $W_C$ ). The electrode porosity,  $\epsilon$ , was calculated according to the equation:

$$\epsilon = \frac{W_B - W_A}{W_B - W_C} \frac{\rho_{\text{H}_2\text{O}}}{\rho_o} \times 100\% \quad (1)$$

where  $\rho_{\text{H}_2\text{O}}$  and  $\rho_o$  are the densities of water and oil, respectively, at the test temperature.

### *Cell design and operation*

A carbon positive was combined with a lithium-foil negative of the same size in a container made from pyrex glass. The two electrodes were separated by glass fibre which had a good chemical resistance and readily allowed the diffusion of ions. The electrolyte comprised 30 ml of  $\text{LiAlCl}_4/\text{SOCl}_2$  or  $\text{AlCl}_3/\text{SOCl}_2$ .

The cell was discharged under constant current (5 - 100  $\text{mA cm}^{-2}$ ) to a voltage cut-off of 2.0 V. The operation was conducted in a glove box filled with argon.

## Results and discussion

### *Effect of electrode porosity*

When the capacity is controlled by the carbon electrode (*i.e.*, "positive-limited" design), the reaction in an Li/SOCl<sub>2</sub> battery is as follows [7]:



The volume change of the electrode solid phase,  $\Delta v$ , due to discharging is given by:

$$\Delta v = v_{\text{LiCl}}(It/nF) \quad (3)$$

where  $n = 1$  and  $v_{\text{LiCl}}$  is the product of the molar volume of LiCl and the number of moles. Note that LiCl is the solid product formed on discharging and will accumulate on the carbon electrode. The discussion presented here ignores the possibility that sulphur might also be deposited on the carbon electrode [3].

The volume of the carbon electrode before cell discharge is given by:

$$v_i = (m_c/\rho_c)/(1 - \epsilon_i) \quad (4)$$

where  $\epsilon_i$  is the initial porosity,  $m_c$  is the weight, and  $\rho_c$  is the true density of the carbon electrode. After cell discharge, the volume of the carbon electrode becomes:

$$v_f = \{(m_c/\rho_c) + v_{\text{LiCl}}(It/F)\}/(1 - \epsilon_f) \quad (5)$$

where  $\epsilon_f$  is the resulting porosity of the carbon electrode. Since the charge passed,  $Q$ , is given by:

$$Q = It \quad (6)$$

substitution of eqns. (4) and (5) in eqn. (6) yields:

$$Q = \left\{ \frac{\epsilon_i - [1 - v_f/v_i(1 - \epsilon_f)]}{(1 - \epsilon_i)} \right\} \{F/v_{\text{LiCl}}\} \{m_c/\rho_c\} \quad (7)$$

Therefore, the electrode capacity per unit weight,  $C_p$ , is given by:

$$\begin{aligned} C_p &= \left\{ \frac{\epsilon_i - [1 - v_f/v_i(1 - \epsilon_f)]}{(1 - \epsilon_i)} \right\} \{1/v_{\text{LiCl}}\} \{F/\rho_c\} \\ &= K \left\{ \frac{\epsilon_i - [1 - v_f/v_i(1 - \epsilon_f)]}{(1 - \epsilon_i)} \right\} \end{aligned} \quad (8)$$

where  $K = (1/v_{\text{LiCl}})(F/\rho_c)$ .

If it is assumed that the change in volume of the electrode during cell discharge is negligible, *i.e.*,  $v_f \approx v_i$ , then eqn. (8) can be simplified to:

$$C_p = K\{(\epsilon_i - \epsilon_f)/(1 - \epsilon_i)\} \quad (9)$$

Since  $\epsilon_f$  is usually between 0.1 and 0.2 [8], the electrode capacity,  $C_p$ , is given by:

$$C_p = K\{(\epsilon_i - 0.1)/(1 - \epsilon_i)\} \quad (10)$$

Using the above equations, the cell capacity can be estimated from measurements of the electrode porosity. Since the latter is sensitive to both the pressure and the content of PTFE used in the preparation of the electrodes, the effects of these two parameters will naturally be of great interest.

*Effect of pressure.* During the manufacture of carbon electrodes, high pressures can result in a decrease in the spaces not only between the carbon particles, but also in the thickness of the electrode. Figure 1 and Table 1 summarize the experimental results obtained for electrodes prepared under different pressures and discharged at  $5 \text{ mA cm}^{-2}$ . The data demonstrate an inverse relationship between pressure and both electrode porosity and capacity. However, if the pressure is too low, *i.e.*, below  $10 \text{ kg cm}^{-2}$ , the electrode structure is loose and is impractical for use in cells and batteries. Thus,  $10 \text{ kg cm}^{-2}$  is taken to be the optimal manufacturing pressure for the carbon electrode.

When the electrolyte concentration, temperature, and discharge current are kept constant,  $K$  becomes a constant and can be determined from a

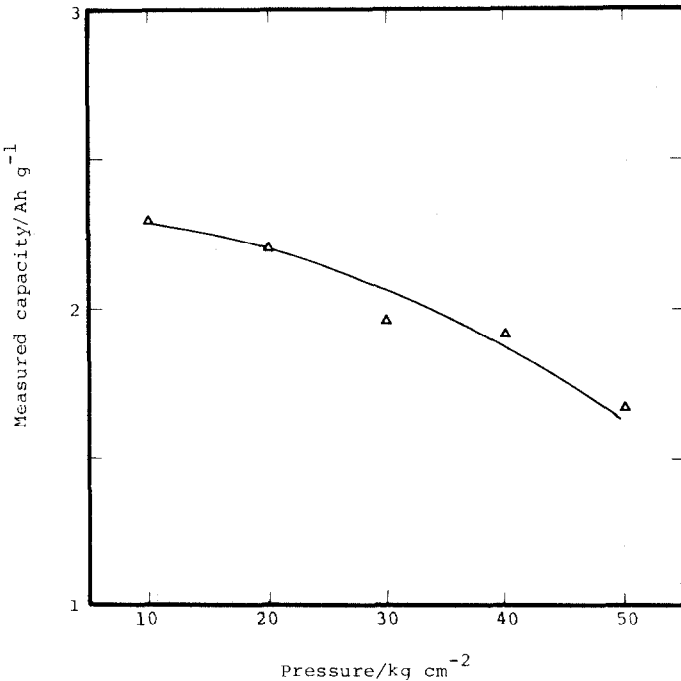


Fig. 1. Relationship between capacity and pressure used in electrode manufacture.

TABLE 1

Relationship between electrode capacity and porosity at various pressures used in electrode manufacture

Pressure (kg cm <sup>-2</sup> )	Initial porosity ( $\epsilon_i$ )	Capacity (A h g <sup>-1</sup> )
10	0.85	2.31
20	0.82	2.20
30	0.80	1.96
40	0.79	1.94
50	0.73	1.67

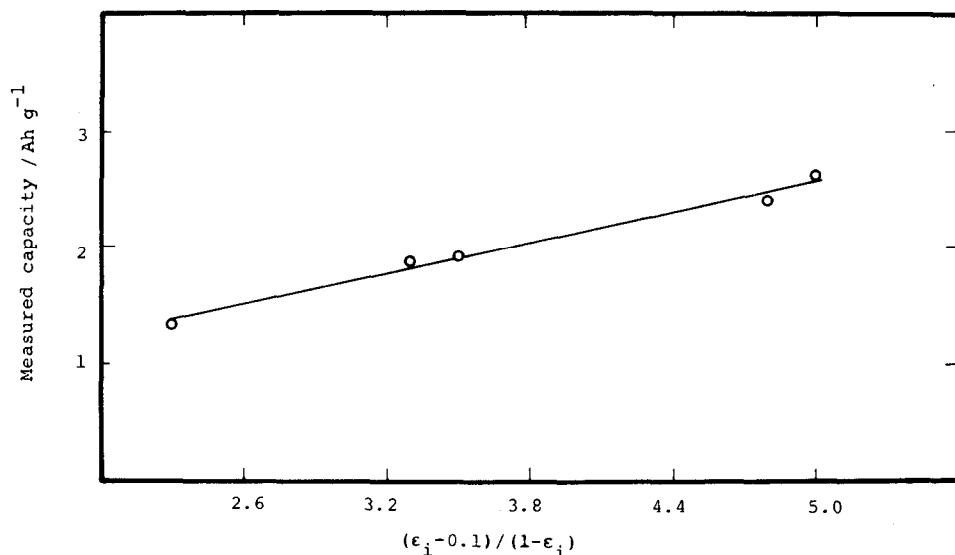


Fig. 2. Relationship between electrode capacity and  $(\epsilon_i - 0.1)/(1 - \epsilon_i)$ .

plot of measured  $C_p$  versus  $(\epsilon_i - 0.1)/(1 - \epsilon_i)$ . The slope obtained is 0.22 according to Fig. 2. But it is apparent from Fig. 2 that  $C_p$  does not approach zero as  $\epsilon_i$  approaches zero. Physically, this means that the electrode maintains a limited amount of discharge capacity even when the electrode has very little porosity. In our system, when  $\epsilon_i = 0.1$ ,  $C_p = 1.19$  A h g<sup>-1</sup>. Therefore, eqn. (10) is modified to:

$$C_p = 0.22\{(\epsilon_i - 0.1)/(1 - \epsilon_i)\} + 1.19 \quad (11)$$

The experimental data of  $C_p$  agree quite well with the calculated values based on eqn. (11) (Fig. 3).

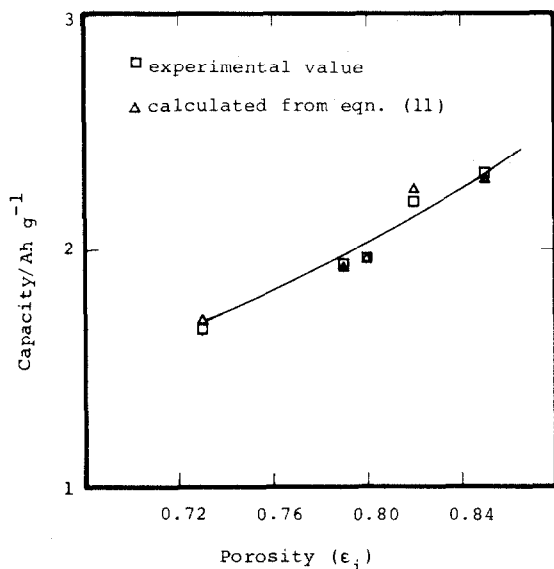


Fig. 3. Relationship between electrode capacity and porosity.

**Effect of PTFE content.** PTFE serves as a binder for the carbon electrode. The influence of PTFE loading on cell capacity is given in Fig. 4. The data clearly show that the capacity decreases as the content of PTFE increases; this is because not only is there a proportional decrease in the amount of carbon powder, but also the porosity of the electrode is reduced. Consequently, there is less surface area for the deposition of LiCl.

A PTFE content of 5 wt.% was chosen, as below this value the electrode had poor quality and was subject to shedding problems.

#### *Reaction mechanisms of $\text{AlCl}_3/\text{SOCl}_2$ and $\text{LiAlCl}_4/\text{SOCl}_2$ systems*

The electrode capacities and the polarization curves of cells containing  $\text{AlCl}_3$  or  $\text{LiAlCl}_4$  electrolytes are compared in Figs. 5 and 6, respectively. The data demonstrate that both the electrode capacity and the cell voltage are greater with the  $\text{AlCl}_3$  electrolyte.

The passivating multilayer LiCl film on the surface of the Li anode can be dissolved in an  $\text{AlCl}_3$  electrolyte. Consequently, the voltage delay at the lithium electrode is reduced and the porosity of the carbon electrode is maintained at the initial (high) value. However, it should be noted that the use of an  $\text{AlCl}_3/\text{SOCl}_2$  electrolyte can result in corrosion of the lithium electrode.

The reduction mechanisms of  $\text{AlCl}_3/\text{SOCl}_2$  and  $\text{LiAlCl}_4/\text{SOCl}_2$  electrolytes have been compared through conducting cyclic voltammetric studies on a cell consisting of platinum working ( $0.5 \times 0.5$  cm) counter and reference electrodes. The results obtained for different scan rates in a 3.0 M

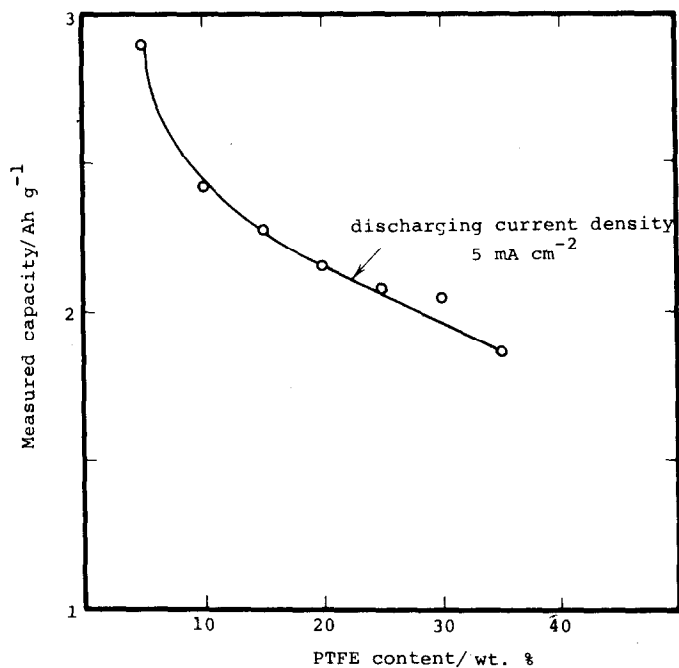


Fig. 4. Relationship between electrode capacity and PTFE content.

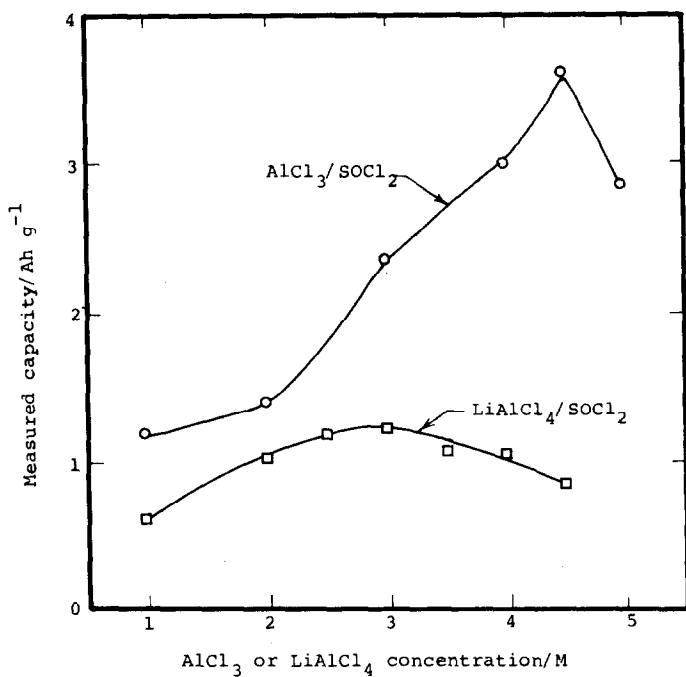


Fig. 5. Relationship between the electrode capacity and electrolyte concentration.

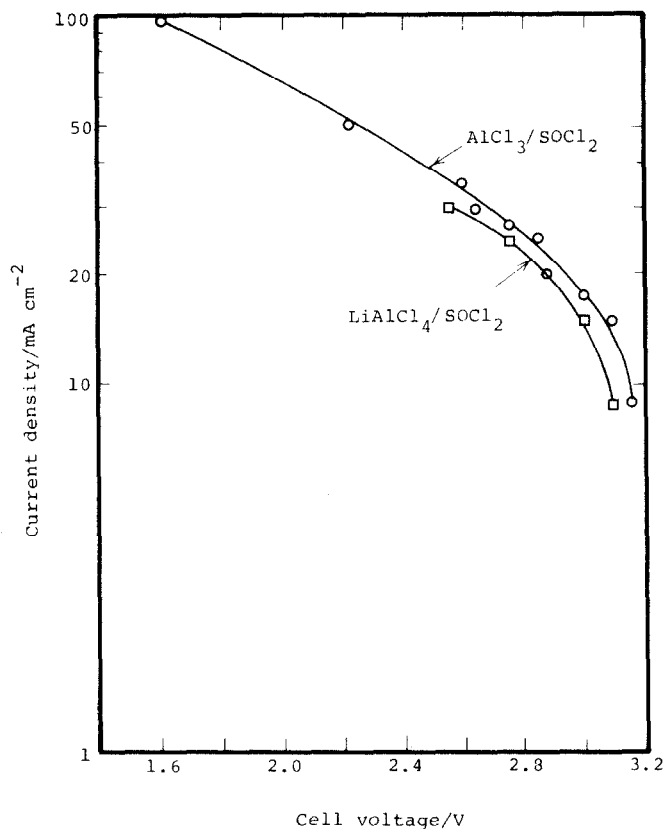


Fig. 6. Relationship between discharging current density and cell voltage.

LiAlCl<sub>4</sub>/SOCl<sub>2</sub> electrolyte system are given in Fig. 7. The voltammograms show the presence of two reduction peaks on the cathodic scan. The potentials ( $E_p$ ) of these peaks shift with change in the scan rate. Two peaks were also observed in the anodic scan. According to reports in the literature [9, 10], the two cathodic peaks are the reduction reactions of SOCl<sub>2</sub> and SOCl, while the two anodic peaks are the corresponding oxidation reactions. Cyclic voltammetric studies also indicate that the reduction reactions are irreversible in the LiAlCl<sub>4</sub>/SOCl<sub>2</sub> electrolyte system.

Cyclic voltammograms for a 4.5 M AlCl<sub>3</sub>/SOCl<sub>2</sub> system are given in Fig. 8. In this case, there is only one reduction peak and no oxidation peaks. Thus, the reduction of SOCl<sub>2</sub> in the AlCl<sub>3</sub>/SOCl<sub>2</sub> system is totally irreversible.

A detailed mathematical analysis of the shape of the voltammograms for reversible and irreversible electrochemical reactions followed by chemical reactions has been given by Nicholson and Shain [11]. One of the diagnostic criteria is a plot of  $i_p/\nu^{1/2}$  against  $\nu$ , where  $i_p$  is the peak current and  $\nu$  is the scan rate. Venkatesetty [12] treated the SOCl<sub>2</sub>/aprotic-organic-solvent system successfully according to this diagnostic criterion.



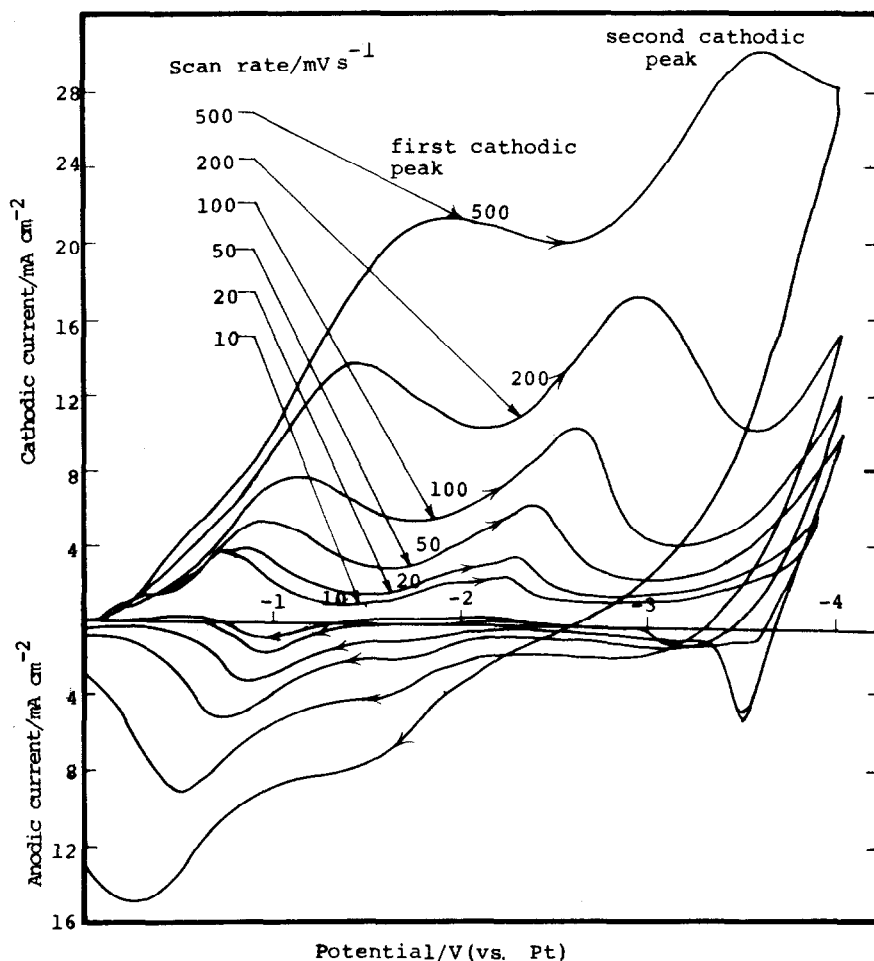


Fig. 7. Cyclic voltammograms for a platinum electrode in 3.0 M  $\text{LiAlCl}_4/\text{SOCl}_2$  at given scan rates.

Similar relationships have been found in the  $\text{AlCl}_3/\text{SOCl}_2$  system (Fig. 9). It can be concluded that the results are consistent with an irreversible charge-transfer reaction followed by a chemical reaction. Therefore, the reduction mechanism of  $\text{SOCl}_2$  in an  $\text{AlCl}_3/\text{SOCl}_2$  system can be characterized by the following steps:



For an irreversible electrochemical reaction that is controlled by the rate of mass transport, the following equation [13] applies:

$$i_p = 3.01 \times 10^5 n(\alpha n_\alpha)^{1/2} A C_o D_o^{1/2} \nu^{1/2} \quad (14)$$

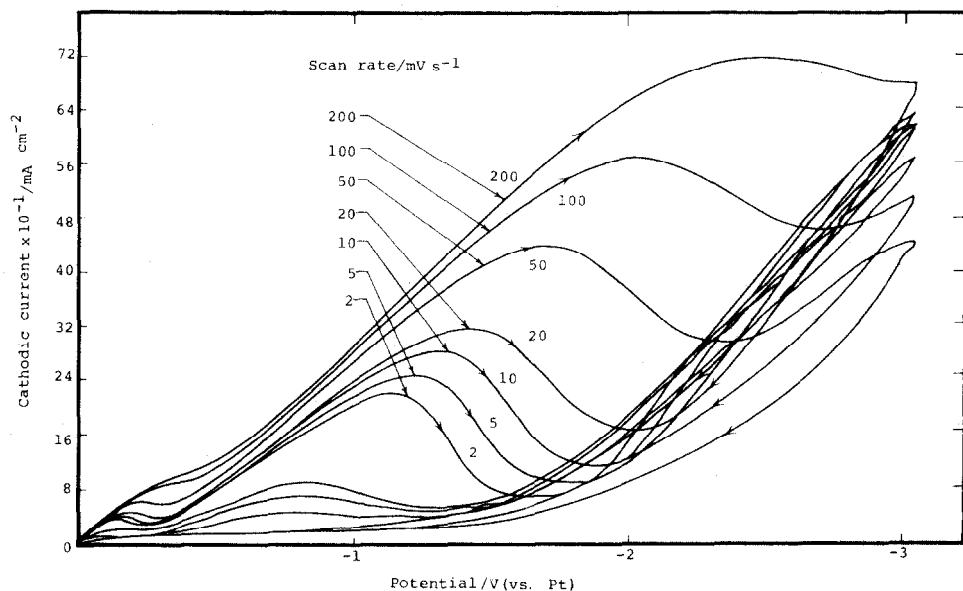


Fig. 8. Cyclic voltammograms for a platinum electrode in 4.5 M  $\text{AlCl}_3/\text{SOCl}_2$  at given scan rates.

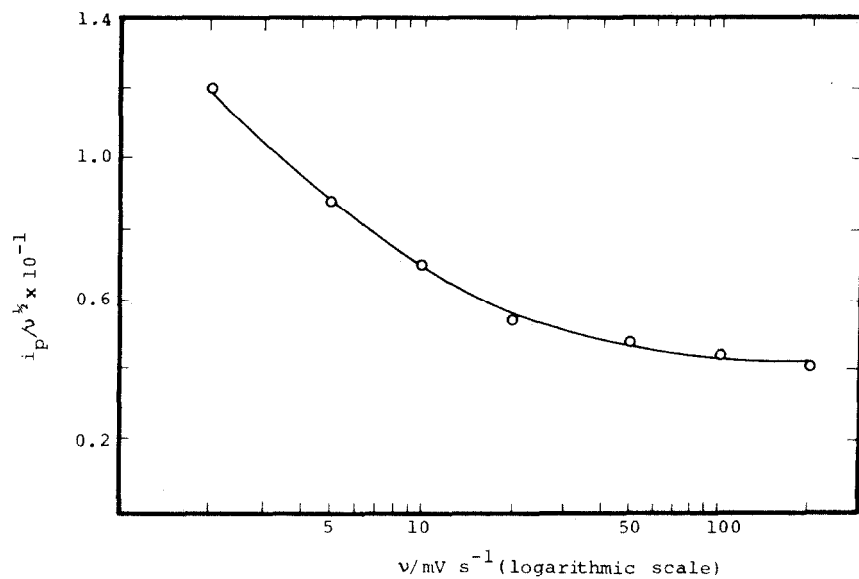


Fig. 9. Relationship between  $i_p/v^{1/2}$  and  $v$  for an  $\text{AlCl}_3/\text{SOCl}_2$  system.

where  $n$  is the number of electrons transferred,  $\alpha$  is the electron transfer coefficient,  $n_\alpha$  is the number of electrons transferred in the rate-determining step,  $C_o$  is the electrolyte concentration, and  $D_o$  is the diffusion coefficient. Plots of  $i_p$  versus  $v^{1/2}$  show (Fig. 10) that the reduction reactions of  $\text{SOCl}_2$

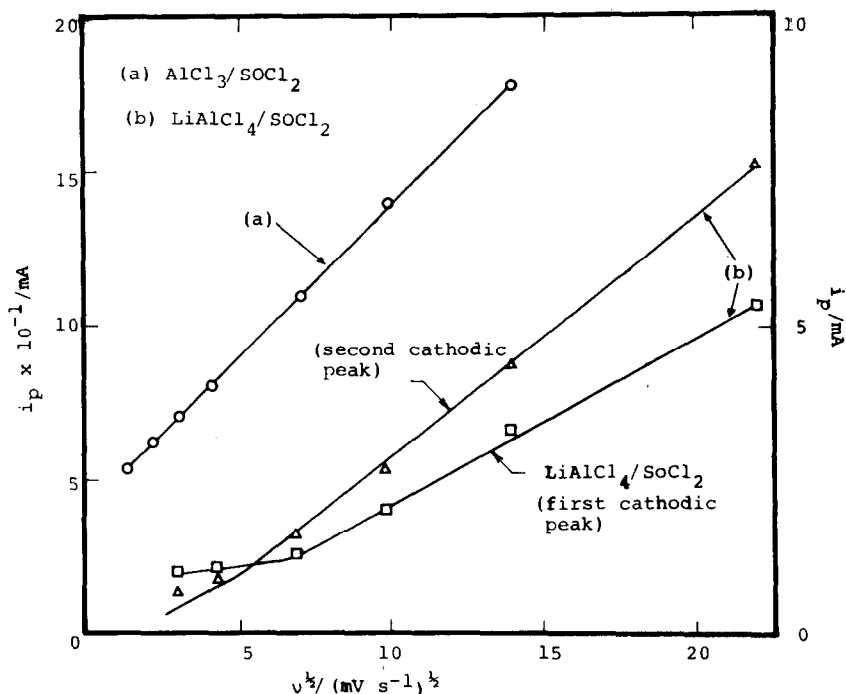


Fig. 10. Relationship between  $i_p$  and  $\nu^{1/2}$  for (a)  $\text{AlCl}_3/\text{SOCl}_2$  and (b)  $\text{LiAlCl}_4/\text{SOCl}_2$  systems.

in 4.5 M  $\text{AlCl}_3/\text{SOCl}_2$  and 3.0 M  $\text{LiAlCl}_4/\text{SOCl}_2$  systems are subject to mass-transport control over scan-rate ranges of 2 - 200  $\text{mV s}^{-1}$  and 20 - 500  $\text{mV s}^{-1}$ , respectively.

For a mass-transfer controlled reaction, the dependence of the peak potential,  $E_p$ , on the scan rate,  $\nu$ , is given by [13]:

$$E_p = \text{constant} - \frac{RT}{2\alpha n_\alpha F} \ln \nu \quad (15)$$

The component  $\alpha n_\alpha$  can be obtained from the slope of a plot of  $E_p$  versus  $\ln \nu$ , i.e., in Fig. 11. By substituting  $\alpha n_\alpha$  into eqn. (14), the diffusion coefficient ( $D_o$ ) can be calculated. The value of  $D_o$  is found to be about  $10^{-10}$  -  $10^{-12}$   $\text{cm}^2 \text{s}^{-1}$  for the  $\text{LiAlCl}_4/\text{SOCl}_2$  system and  $10^{-6}$   $\text{cm}^2 \text{s}^{-1}$  for the  $\text{AlCl}_3/\text{SOCl}_2$  system. If mass-transport control occurs in the liquid phase, then the value of  $D_o$  should be around  $10^{-5}$  -  $10^{-6}$   $\text{cm}^2 \text{s}^{-1}$  [14], i.e., the value found for the  $\text{AlCl}_3/\text{SOCl}_2$  electrolyte. On the other hand, the value of  $D_o$  should be approximately  $10^{-8}$  -  $10^{-10}$   $\text{cm}^2 \text{s}^{-1}$  [14] for mass-transport control in a solid phase. Judging from the value of  $D_o$  obtained for the  $\text{LiAlCl}_4/\text{SOCl}_2$  system, it appears that in this case reduction of  $\text{SOCl}_2$  proceeds via mass-transport control in the solid phase. The solid phase presumably consists of the reduction product. The fact that mass transport

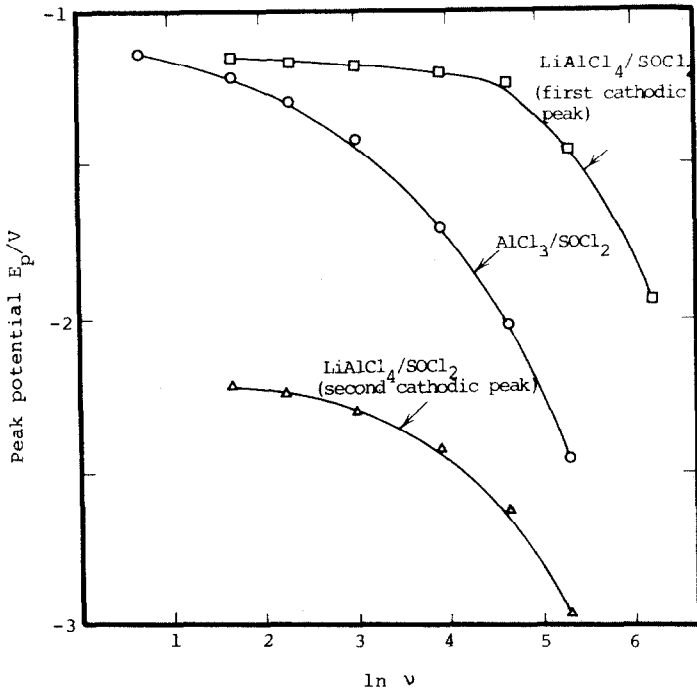


Fig. 11. Relationship between  $E_p$  and  $\ln \nu$ .

occurs in the liquid phase in an  $\text{AlCl}_3/\text{SOCl}_2$  electrolyte system is probably because the electrolyte can dissolve the product of  $\text{SOCl}_2$  reduction on the electrode.

## Conclusions

The following conclusions can be drawn from the data obtained from these studies.

(i) The electrode capacity of an  $\text{Li}/\text{SOCl}_2$  battery system is sensitive to the porosity of the carbon electrode. A semi-empirical equation can be developed to predict the electrode capacity. Moreover, the porosity of the carbon electrode can be controlled during the manufacturing process by applying different pressures and different contents of PTFE binder. The recommended conditions are  $10 \text{ kg cm}^{-2}$  pressure and 5 wt.% PTFE.

(ii) The reduction of  $\text{SOCl}_2$  in both the  $\text{AlCl}_3/\text{SOCl}_2$  and  $\text{LiAlCl}_4/\text{SOCl}_2$  electrolytes is mass-transport controlled for scan rates in the  $2 - 200 \text{ mV s}^{-1}$  and the  $20 - 500 \text{ mV s}^{-1}$  ranges, respectively.

(iii) Since the  $\text{AlCl}_3/\text{SOCl}_2$  electrolyte can dissolve the product from the reduction of  $\text{SOCl}_2$ , the mass-transport phenomenon occurs in the liquid phase with a diffusion coefficient of about  $10^{-6} \text{ cm}^2 \text{ s}^{-1}$ . On the other hand,

in an  $\text{LiAlCl}_4/\text{SOCl}_2$  electrolyte, the process occurs in the solid phase with a diffusion coefficient of approximately  $10^{-10} - 10^{-12} \text{ cm}^2 \text{ s}^{-1}$ .

## References

- 1 C. R. Schlaikjer, in J. P. Gabano (ed.), *Lithium Batteries*, Academic Press, London, 1983, p. 304.
- 2 N. Marincic, *J. Appl. Electrochem.*, 6 (1976) 463.
- 3 A. N. Dey, *J. Electrochem. Soc.*, 123 (1976) 1262.
- 4 S. Szpak and J. R. Driscoll, *J. Power Sources*, 10 (1983) 343.
- 5 K. A. Klinedinst, *J. Electrochem. Soc.*, 132 (1985) 2044.
- 6 C. W. Walker, Jr., M. L. Wade, Jr. and S. Gilman, *J. Electrochem. Soc.*, 132 (1985) 1536.
- 7 J. P. Gabano, *French Pat. 2,079,744* (1971).
- 8 K. Micka, I. Rousar and J. Jindra, *Electrochim. Acta*, 23 (1978) 1031.
- 9 W. K. Behl, *Proc. 27th Power Sources Symp.*, The Electrochemical Society Inc., Pennington, NJ, 1976, p. 30.
- 10 K. M. Abraham and R. M. Mark, *Proc. 29th Power Sources Symp.*, The Electrochemical Society Inc., Pennington, NJ, 1980, p. 135.
- 11 R. S. Nicholson and I. Shain, *Anal. Chem.*, 36 (1964) 706.
- 12 H. V. Venkatesetty, *J. Electrochem. Soc.*, 127 (1980) 2531.
- 13 P. Delahay, *New Instrumental Methods in Electrochemistry*, Interscience Publishers, Inc., New York, 1954, pp. 126 - 128.
- 14 C. O. Bennet, *Momentum, Heat and Mass Transfer*, McGraw-Hill, New York, 1982.